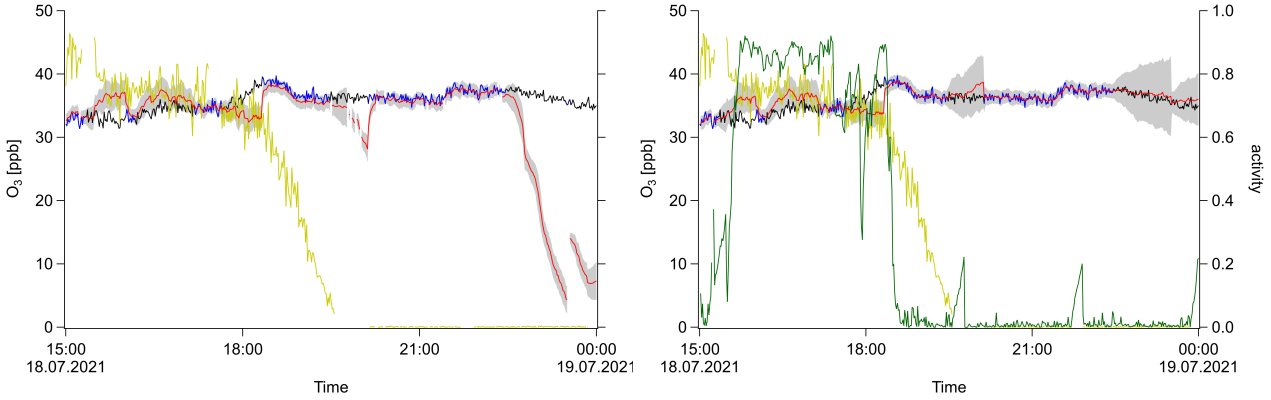

Figure S1. Visualization of the effect of the activity parameter η. The SMC shows undesired behavior when data is missing and the provided transition function does not correspond to the dominant system dynamics. This problem is shown on an example of the SMC used for interpolation of ozone. O_3 mixing ratio as a function of time (UTC) for an arbitrary day of the field campaign. Original measurement (black), measurement with artificial gaps (blue), PSS calculation (yellow), SMC ensemble mean (red) and $\pm 1\sigma$-interval (shaded grey region). Top: The basic algorithm described in section 3.1 without activity parameter η is used. When ozone data is missing during the night, the algorithm quickly decreases the resulting mixing ratio to values close to the PSS. Bottom: The extended algorithm 1 with activity parameter η is used. Its average value is plotted in green. At sunset the system becomes passive and the algorithm does not use the provided chemistry anymore. The stochastic part of the prior dominates and ozone no longer vanishes where no data is provided.

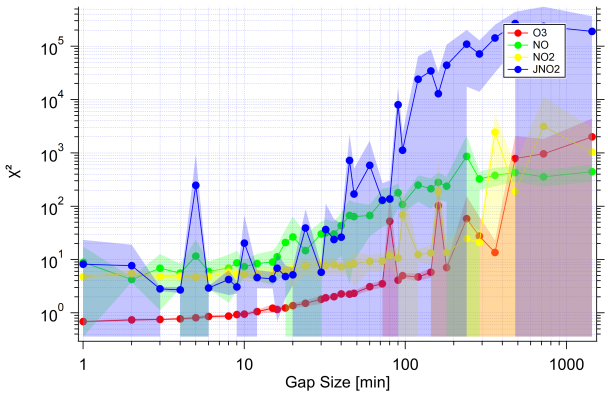

Figure S2. χ^2 of the SMC estimation as a function of artificial data gap size to study the interpolation capabilites. Mean χ^2 as lines and markers and standard deviation as shaded region for the ensemble of repetitions. The plot shows the results of all variables ozone (red), NO (green), NO_2 (yellow) and j_{NO_2} (blue).

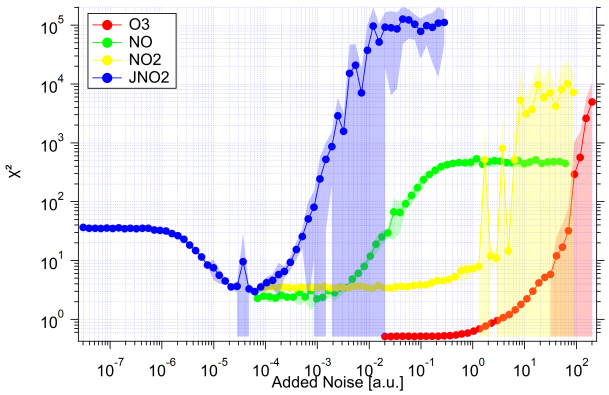

Figure S3. χ^2 of the SMC estimation a function of artificial noise to study the precision enhancement abilities. Mean χ^2 as lines and markers and standard deviation as shaded region for the ensemble of repetitions. The plot shows the results of all variables ozone (red), NO (green), NO_2 (yellow) and j_{NO_2} (blue).

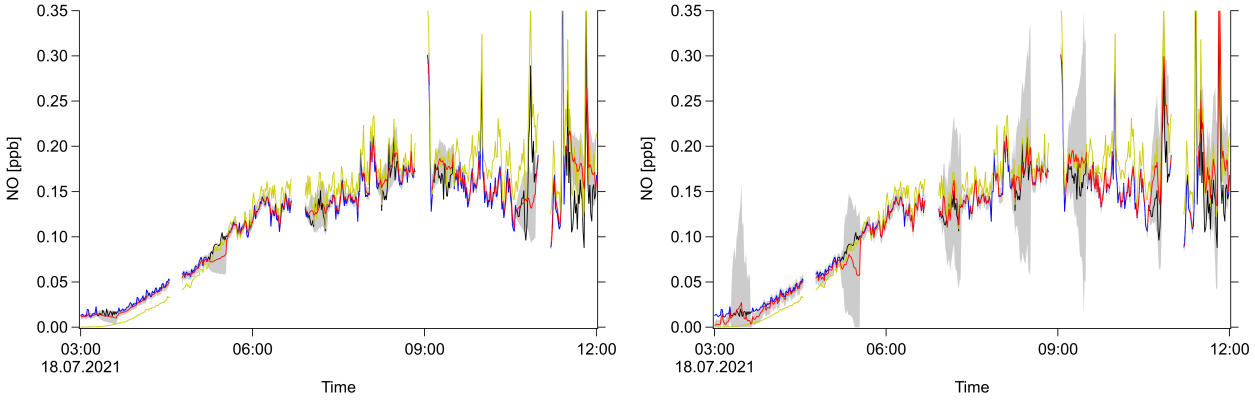

Figure S4. Variation of the free parameter σ_0 and its exemplary effect on the interpolation of NO. $\sigma_{0,\mathrm{const}}$ is decreased (top) and increased (bottom) by a factor of 10. NO mixing ratio as a function of time (UTC) for an arbitrary day of the field campaign. Original measurement (black), measurement with artificial gaps (blue), PSS calculation (yellow), SMC ensemble mean (red) and $\pm 1\sigma$-interval (shaded grey region).

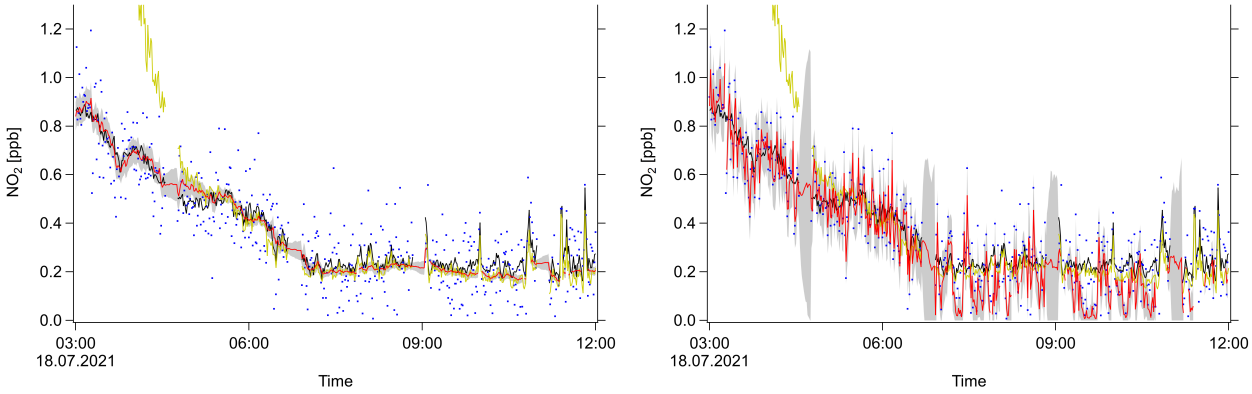

Figure S5. Variation of the free parameter σ_0 and its exemplary effect on the denoising of NO_2. $\sigma_{0,\mathrm{const}}$ is decreased (top) and increased (bottom) by a factor of 10. NO_2 mixing ratio as a function of time (UTC) for an arbitrary day of the field campaign. Original measurement (black), measurement with artificial noise (blue), PSS calculation (yellow), SMC ensemble mean (red) and $\pm 1\sigma$-interval (shaded grey region).

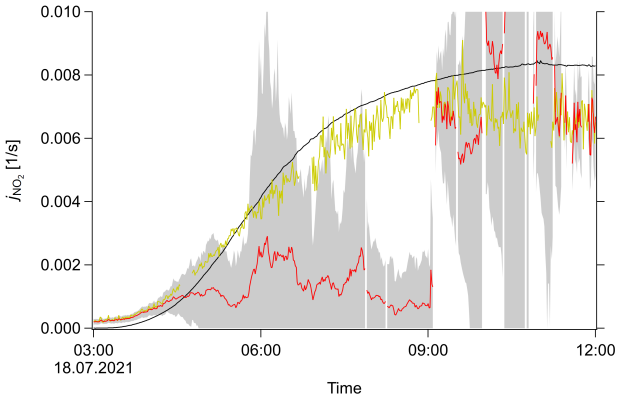

Figure S6. Variation of the free parameter σ_0 and its exemplary effect on the inference of $j_{\mathrm{NO_2}}$. $\sigma_{0,\mathrm{rel}}$ is increased by a factor of 3. Photolysis frequency j as a function of time (UTC) for an arbitrary day of the field campaign. Original measurement (black), PSS calculation (yellow), SMC ensemble mean (red) and $\pm 1\sigma$-interval (shaded grey region).

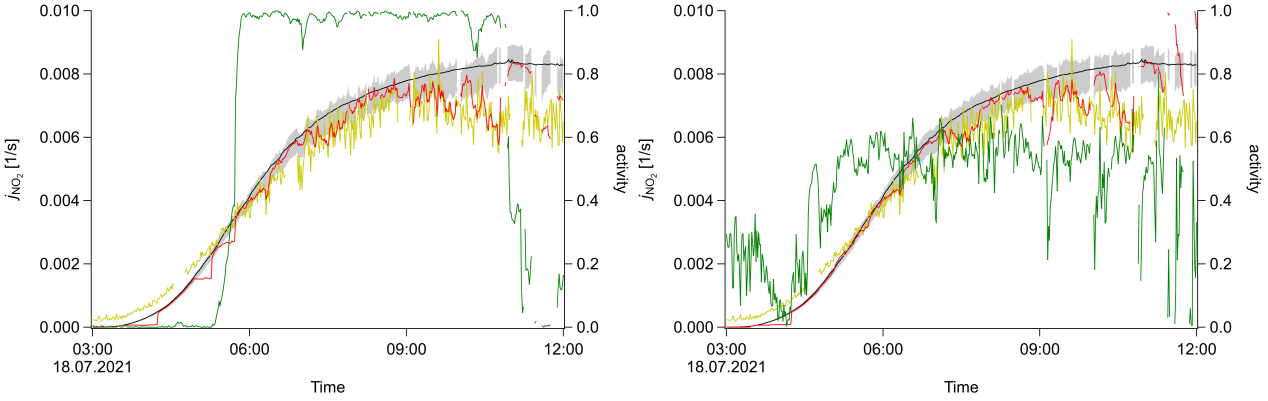

Figure S7. Variation of the free parameter p_η and its exemplary effect on the interpolation of $j_{\mathrm{NO_2}}$. p_η is decreased (top) and increased (bottom) by a factor of 10. Photolysis frequency j as a function of time (UTC) for an arbitrary day of the field campaign. Original measurement (black), measurement with artificial gaps (blue), PSS calculation (yellow), SMC ensemble mean (red) and $\pm 1\sigma$-interval (shaded grey region), average activity (green).

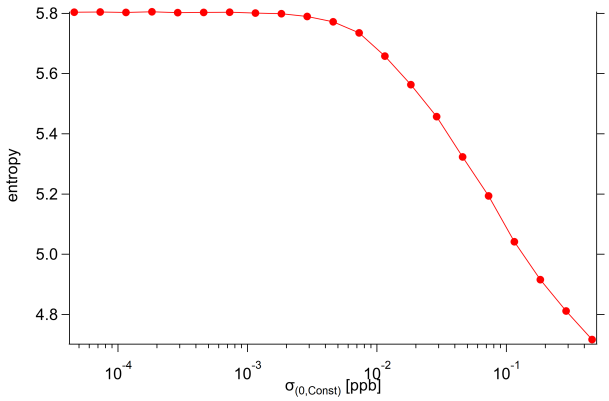

Figure S8. Variation of the free parameter $\sigma_{0,\mathrm{const}}$ and its exemplary effect on the interpolation of NO. The median entropy is plotted for several runs as a function of each free parameter setting.

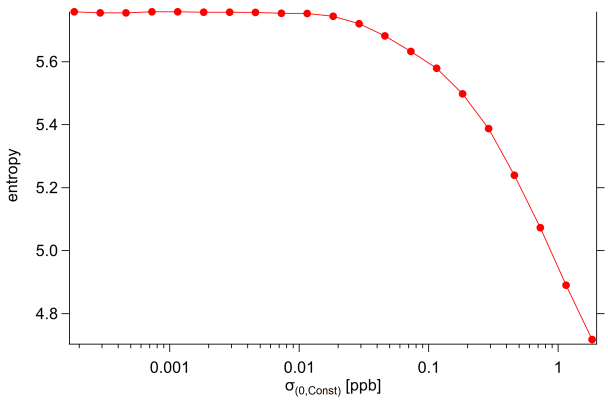

Figure S9. Variation of the free parameter $\sigma_{0,\mathrm{const}}$ and its exemplary effect on the denoising of NO_2. The median entropy is plotted for several runs as a function of each free parameter setting.

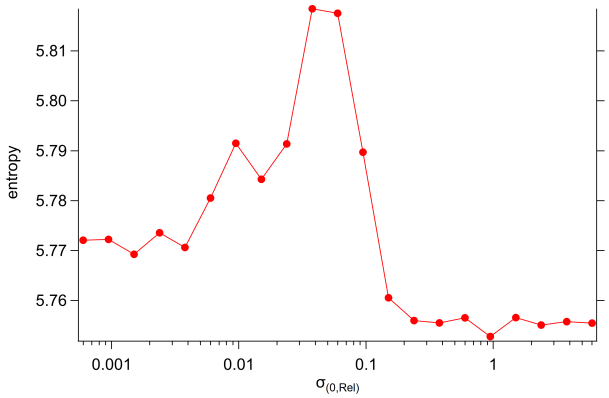

Figure S10. Variation of the free parameter $\sigma_{0,\mathrm{rel}}$ and its exemplary effect on the inference of $j_{\mathrm{NO_2}}$. The median entropy is plotted for several runs as a function of each free parameter setting. In this particular case the entropy shows a maximum and decreases again with lower σ_0.

Variable	Detection Limit	Precision [%]	$\sigma_{0,\mathrm{const}}$	$\sigma_{0,\mathrm{rel}}$ [%]
O_3	2 ppbv	2	0.68 ppbv	0.3
NO	7 pptv	4	4.6 pptv	6.6
NO_2	10 pptv	12	18 pptv	2.7
jNO_2	$3 \cdot 10^{-6}\ \mathrm{s}^{-1}$	10	$1.5 \cdot 10^{-5}\ \mathrm{s}^{-1}$	6

Table S1. System parameters used throughout the study. Detection Limit and Precision are taken from the measurement datasets. Note that the photolysis frequency is only calculated from solar radiation. The contribution from diffuse radiation is not considered. The σ_0 parameters are retrieved from linear fits of the difference between consecutive measurements vs the measurement value. Additional parameters are the switching probability $p_\eta = 2.5\%$, the ensemble size $K = 1000$ and the auxiliary ensemble size $R = 10000$.